

STUDY IN MICROWAVE RANGE OF SOME HF BOARD MATERIALS FOR LEAD-FREE TECHNOLOGIES

D. IONESCU¹, I.B. CIOBANU²

^{1,2}“Gh. Asachi” Technical University of Iași, Romania, ¹Faculty of Electronics and Telecommunications, 11 Carol I Blvd., 700506 Iași, RO, E-mail: danaity@yahoo.com

²Department of Physics, 67 D. Mangeron Blvd., 700050 Iași, RO, Email: bciobanu2003@yahoo.com

(Received September 2, 2008)

Abstract. A simulation strategy for complex structures with multiple components was developed and employed in this paper. The analyzed materials were represented by a category of substrate materials for printed circuit boards, used in lead-free design at high exploitation frequencies. The frequency evolution of properties of these materials was analyzed in the frequency range of 0.3 to 7.4 GHz, considering a material parameter: the effective electric permittivity, ϵ_r . This quantity was determined from considerations of energy variations at material polarization, induced by an external field E . Different material samples were simulated with the help of a dedicated program (High Frequency Structural Simulator, HFSS-Ansoft Technologies) used for high frequency (HF) material analyses. Results are available for concluding on different materials behavior in HF and microwave fields, in order to formulate their optimal employment strategy.

Key words: lead-free board materials, structural simulation, multi-components structure, energy variations, effective permittivity, electrical resonances, microwave range.

1. INTRODUCTION

The electrical characteristics of the printed circuit board (PCB) structural components, in a high-frequency product, influence strongly the product performance. For determining the electric properties by simulation or modeling, software packages are available [3, 4, 5]. Their working strategy is based on modeling methods like:

– Method of Moments (MOM) – applied for analyzing the radiated electric field of PCB emissions caused by the common mode currents on the enclosure/box, connectors, and cables; a structure is usually divided into segments with dimensions much smaller than the signal wavelength; discrete components are easily inserted into a model as impedance assignments to a given wire segment; the main disadvantage of MOM: it is difficult to be applied for aperture effects and for dielectric materials.

– Finite Difference Time Domain (FDTD), for the simulation of a PCB and its associated components and connectors within the interior of the shielded enclosure or box; it is a time domain technique; using FDTD one determines the *E*-fields and *H*-fields within the defined simulation space cells, which can consist of any material such as air or free space, metal and dielectrics; computational domain grid has to be much smaller than the smallest wavelength and sample feature; method disadvantage: it may not be applicable for far fields determination and in the case of some samples with extended features such as wires.

– Uniform Theory of Diffraction (UTD) is useful for direct rays, reflected rays, diffractions from edges and corners, and waves around curved surfaces determinations; uses modeling elements of flat plates, cylinders of elliptical cross-section, and the end caps of each cylinder that may be tilted.

– Frequency Domain Finite Differences (FDFD or FD) gives the electromagnetic fields components at points in closed regions using a specialized form of Householder's Method of Modified Matrices; FD boundaries are specified by the UTD modeling elements.

– Electrical models representing PCB structures, considering the parasitic elements on PCB (equivalent circuit method), responds perfect to the requirement for increased inclusion of electrical models representing PCB structures into the circuit simulation.

Because of circuit and structure complexity, a multiple stage modeling or simulation suite is most efficient in dealing with all the different PCB design problems. Examples of such combined modeling techniques may be the following:

– MOM/UTD – for modeling structures that usually requires MOM matrix methods and UTD ray tracing for achieving solutions. An example of a MOM/UTD hybrid is a monopole antenna (MOM segments) attached to a finite size ground plane (UTD plate).

– MOM/UTD/FD – for modeling testing structures with more than one region, such as an interior and an exterior. FD is used to model the interior region(s), while MOM or MOM/UTD is used to model the exterior region. The physics of each region is reduced to a matrix format with boundary conditions across the areas.

We have exploited here one of the software packages that combine suitable techniques for an efficient operational PCB analysis: the High Frequency Structure Simulator (HFSS-Ansoft Technologies). With help of the HFSS, complex 3D geometries for microwave/RF frequencies were modeled using the finite-element method (FEM).

Why HFSS? Because the frequency-dependent material properties can be critical at microwave/millimeter-wave frequencies and the program can determine a fairly complete frequency evolution of the material parameters, including the resonances. The program allows to the users to specify very general mathematical expressions for complex material properties, on order to define the frequency-

dependent material, and the software automatically performs a complete and detailed analysis over frequency, which dramatically reduces the engineering time. In this context, the FR4 and other common PCB laminates, for example, are comprised of glass fibers and epoxy resin. The electric permittivity of the resin varies with frequency, as does the loss tangent of the glass. The impedance of printed lines depends directly on the electric permittivity of the surrounding layers of laminate. This frequency-dependent effect has to be considered for efficient controlled impedance designs, regardless of whether single-ended lines or differential pairs are used. Manufacturers of PCB laminates typically specify electric permittivity and loss tangent near DC and at a moderate microwave frequency. Supplementary determinations are necessary, considering a frequency sweeping. In the same time, the material parameters frequency behavior is a resonant one. Each resonance represents a break-up of the electric properties, with a considerable magnitude modification of the material parameters. That is why resonances are to be avoided or have controlled exploitation, depending on the material usage imposed task.

Lead-Free Design for electronic printed circuit boards (PCB), in agreement with European standards, emphasizes the necessity of halogen-free materials for PCB substrates (i.e. see the IEC 61249-2-21). Other major needs for PCB are: *high frequency characteristics*; high reliability; workability [14, 15].

We have considered here for analysis the recommended PCB materials [1, 6, 7]:

For multi-layer PCB:

1) Low Dk and high Tg material MEGTRON6, double-sided copper clad, R-5775(K); (Prepreg R-5670 (K));

(Dk = dielectric constant, which represents the effective permittivity in DC; Tg = glass transition temperature)

2) Low Dk and high Tg material MEGTRON Plus, double-sided copper clad, R-5715T (Prepreg R-5610T) (grade FR-4);

3) Low Dk and high Tg material MEGTRON2, double-sided copper clad, R-5715(J) (Prepreg R-5715(P)) (grade FR-4);

4) MEGTRON PreMulti (Masslam) C-5810 (also similar: PreMulti (Masslam) C-1810) (grade FR-4).

For double-sided PCB:

5) Glass PTFE (polytetrafluoroethylene) Copper-clad laminate, R-4737;

6) Glass thermosetting PPO (poly-p-phenylene oxide) resin copper-clad laminate (low Dk type), R-4726;

7) Glass thermosetting PPO resin copper-clad laminate (high Dk type), R-4728.

The electrical properties of these materials were analyzed, in the high frequency range of 0.3 to 7.4 GHz, where the most of resonances are present with magnitudes high enough to be considered. PCB materials frequency behavior was illustrated by effective permittivity determinations, which present resonant evolution with frequency in microwave range [8, 9].

The theoretical support for effective permittivity determination, in the case of the considered anisotropic PCB materials, is presented in the considerations below.

2. THEORETICAL CONSIDERATIONS

The considered dielectric materials for PCB substrates are anisotropic. Consequently, when we write the electric induction vector, \mathbf{D} , we have to use the tensor representation of the material electric permittivity (the quantities bold written are 3-D vectors):

$$\mathbf{D} = [\boldsymbol{\varepsilon}] \mathbf{E} = \varepsilon_0 [\boldsymbol{\varepsilon}_r] \mathbf{E}, \quad (1)$$

$$\Leftrightarrow \begin{bmatrix} D_x \\ D_y \\ D_z \end{bmatrix} = \begin{bmatrix} \varepsilon_{11} & \varepsilon_{12} & \varepsilon_{13} \\ \varepsilon_{21} & \varepsilon_{22} & \varepsilon_{23} \\ \varepsilon_{31} & \varepsilon_{31} & \varepsilon_{33} \end{bmatrix} \cdot \begin{bmatrix} E_x \\ E_y \\ E_z \end{bmatrix}, \quad (2)$$

with the electric polarization of the material, \mathbf{P} , given by:

$$\mathbf{P} = \varepsilon_0 [\boldsymbol{\chi}_e] \mathbf{E} = \varepsilon_0 ([\boldsymbol{\varepsilon}_r] - [1]) \mathbf{E}, \quad (3)$$

(with the $[\boldsymbol{\chi}_e]$ tensor represents the material electric susceptibility).

We intend to find the energy variations at material polarization for the anisotropic material case.

For an isotropic dielectric material (with a scalar value for ε_r), exposed to an electrical field \mathbf{E} , the energy variations at material polarization can be written as follows [2]:

$$dW_e = \mathbf{E} \cdot d\mathbf{P}, \quad (4)$$

$$dW_e = (\varepsilon_r - 1) \varepsilon_0 \mathbf{E} \cdot d\mathbf{E} = \frac{1}{2} (\varepsilon_r - 1) \varepsilon_0 \cdot d(\mathbf{E}^2), \quad (5)$$

where the $\varepsilon_0 \varepsilon_r \mathbf{E}^2 / 2$ energy stored in the dielectric material represents: the increased internal energy of the polarized molecules – $\varepsilon_0 (\varepsilon_r - 1) \mathbf{E}^2 / 2$, respectively the energy stored in the vacuum electrical field – $\varepsilon_0 \mathbf{E}^2 / 2$.

If we consider now the anisotropic dielectric material, the relation (4) has to be reconsidered, because of the tensor character of the permittivity, which determines no more alignment between the \mathbf{E} and \mathbf{P} vectors. The derivation operation presents a spatial character, so the tensor affects the derivation result. In this case, the energy variations are:

$$dW_e = \mathbf{E} \cdot d\mathbf{P} = \mathbf{E} \cdot d(\varepsilon_0 [\chi_e] \mathbf{E}). \quad (6)$$

One obtains:

$$dW_e = \varepsilon_0 \cdot (\mathbf{E} \cdot [\chi_e] \cdot d\mathbf{E}). \quad (7)$$

It is important to remark that the result is different from $\varepsilon_0 [\chi_e] (\mathbf{E} \cdot d\mathbf{E})$.

The result can be written as:

$$\begin{aligned} dW_e = & dE_x [(\varepsilon_{11} - 1)E_x + \varepsilon_{21}E_y + \varepsilon_{31}E_z] + \\ & + dE_y [\varepsilon_{12}E_x + (\varepsilon_{22} - 1)E_y + \varepsilon_{32}E_z] + \\ & + dE_z [\varepsilon_{13}E_x + \varepsilon_{23}E_y + (\varepsilon_{33} - 1)E_z]. \end{aligned} \quad (8)$$

If the considered structure has a complex internal structure, the anisotropy axes are difficult to be identified without special determinations. So, the simulations were performed for the real case, when the applied field has a random direction with respect to these axes. But if we apply the external field in order to make the proper field components or variations vanish, the $[\varepsilon]$ tensor components can be determined, with respect to the considered reference system. Permittivity tensor determination is of great interest in practice, because the material presents more than one constituent and the permittivity is an effective one, depending on the kind and geometry of constituents.

3. RESULTS FOR EFFECTIVE PERMITTIVITY IN HF RANGE

Electrical properties of a material depend on the internal structure [12, 13, 15]. Samples of PCB substrate materials no. **1)-7)** were simulated using the HFSS program. Every sample (1.6 mm thickness, Fig. 1) was exposed to a HF electromagnetic field, using a sweeping frequency method, for the frequency range of 0.3 to 7.4 GHz. The components of the effective permittivity tensor were determined for each sample core material when the exposure field had three different directions with respect to sample symmetry axes (the exposure field was not applied on axes). The fact that the same results for tensor components (ε_{11} , ε_{12} , etc.) were obtained (with errors less than 2 %) in every exposure case confirms the viability of the method.

A resonant frequency behavior was found for the anisotropic board materials. Because of material optical anisotropy, if a field propagation direction inside the material is chosen, one obtains two values for the effective relative permittivity ε_r , denoted with $\varepsilon_{||}$, respectively ε_{\perp} . The two values of parallel, respectively transverse permittivity, CAD determined, were represented *versus* frequency for each material sample.



Fig. 1 – Compact different layers of the PCB substrate materials.

For the MEGTRON materials, R-57xx(y) class, the curves of $\epsilon_{||}$ versus frequency are given in Figs. 2 and 3. Similar representations were realized for MEGTRON PreMulti (Masslam), C-5810 class, given on the same figures for comparison. The parallel permittivity curve for the FR-4 standard board material, taken from literature, was also given in Fig. 2, to confirm the decreasing frequency evolution of permittivity for the considered class of materials (grade FR-4). Any resonance is present on the curve for FR-4 because the most of determination methods (theoretical or experimental) can not illustrate the resonances.

The curves representing the ϵ_{\perp} permittivity versus frequency present an increased number of resonances (supplementary resonant frequencies derive from boundary conditions at relative parallel stratification layers edges) and can be illustrated in the same manner (see Fig. 4 for exemplification). Because of the great number of resonances, Table 1 is available in this case. We have to mention that resonances are sharp in practice and their real bandwidth can be precisely determined only by measurements (the simulation program can not give fair results for very many points in resonance neighborhood).

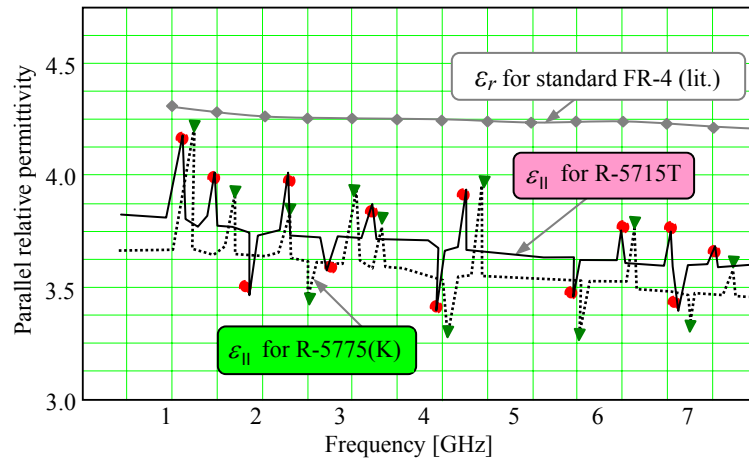


Fig. 2 – The parallel effective permittivities versus frequency, for the R-5775(K) and R-5715T PCB materials, in the frequency range of 0.3-7.4 GHz.

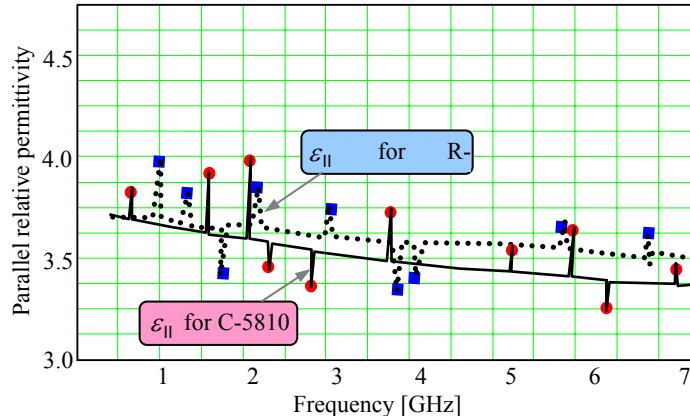


Fig. 3 – The parallel effective permittivities *versus* frequency, for the R-5715(J) and C-5810 PCB materials, in the frequency range of 0.3-7.4 GHz.

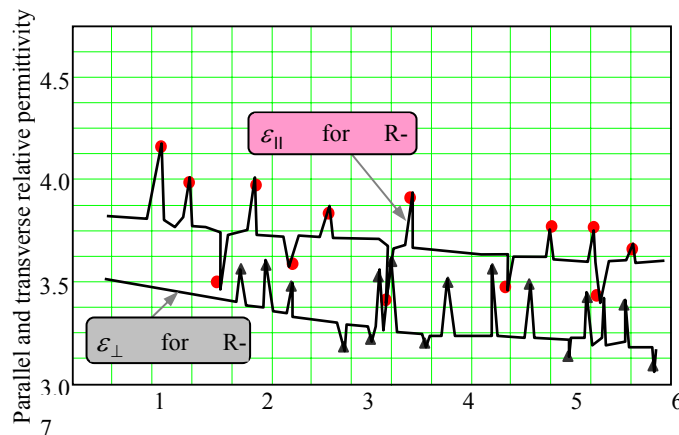


Fig. 4 – The parallel and transverse effective permittivities *versus* frequency, for the R-5715T PCB material, in the frequency range of 0.3-7.4 GHz. Specific resonances are illustrated on both curves.

The graphs indicate the theoretical predicted decreasing with frequency of the effective permittivity, which is more accentuated at lower frequencies in the considered domain (0.3–3 GHz here). The effective permittivity presents resonant peaks and valleys, corresponding to a stronger, respectively weaker effect of polarization inside the material. Considering the relation (1), resonant valleys are associated with a lower field influence on the material and this is a benefit for the exploitation. But the most of resonances are resonant peaks and the corresponding work frequencies have to be avoided. The aim of our method is to find these frequencies, very difficult to be determined by other classical methods [5, 9, 11].

Table 1

Resonant frequencies of the parallel and transverse effective permittivities for the R-57XX(Y) class and for C-5810 PCB materials, in the frequency range of 0.3–7.4 GHz

PCB Material	Resonant Frequencies [GHz]	
	Parallel effective permittivity resonances	Transverse effective permittivity resonances
R-5775(K)	1.228; 1.706; 2.296; 2.593; 3.049; 3.398; 4.221; 4.482; 5.623; 6.178; 6.843; 7.258	2.186; 2.483; 2.965; 3.216; 3.928; 4.098; 4.183; 5.248; 5.396; 5.508; 5.913; 6.002; 6.212; 6.493; 6.594; 7.102; 7.203; 7.406
	<p>On frequency</p> <p>for R-5775(K)</p>	<p>Legend:</p> <p>▼ resonances of</p> <p>↑ resonances</p> <p>of ϵ_{\perp}</p>
R-5715T	1.147; 1.826; 2.254; 2.846; 3.252; 4.086; 4.248; 5.563; 6.014; 6.543; 6.628; 7.085	2.143; 2.463; 2.715; 3.416; 3.682; 3.865; 4.007; 4.432; 4.681; 5.327; 5.749; 6.219; 6.482; 6.667; 6.973; 7.324
	<p>On frequency</p> <p>for R-5715T</p>	<p>Legend:</p> <p>● resonances of</p> <p>↑ resonances</p> <p>of ϵ_{\perp}</p>
R-5715(J)	1.016; 1.324; 1.802; 2.174; 3.102; 3.921; 4.147; 5.832; 6.892	1.643; 1.915; 2.239; 2.414; 2.645; 2.846; 3.024; 3.254; 3.401; 3.715; 3.982; 4.452; 5.613; 5.964; 6.372; 6.684; 7.413
	<p>On frequency</p> <p>for R-5715(J)</p>	<p>Legend:</p> <p>■ resonances of</p> <p>↑ resonances</p> <p>of ϵ_{\perp}</p>
C-5810	0.742; 1.614; 2.094; 2.413; 2.968; 3.802; 5.2846; 6.032; 6.584; 7.289	2.223; 2.496; 2.508; 3.3374; 3.504; 3.792; 4.465; 5.276; 5.489; 5.961; 6.005; 6.615; 6.774; 7.183
	<p>On frequency</p> <p>for C-5810</p>	<p>Legend:</p> <p>● resonances of</p> <p>↑ resonances</p> <p>of ϵ_{\perp}</p>

Board materials considered by us are optical positive (Fig. 4), presenting a positive value for the optical anisotropy:

$$\Delta\varepsilon = \varepsilon_{\parallel} - \varepsilon_{\perp} . \quad (9)$$

This behavior is imposed by the resins nature, which are optical positive in pure state (resin content exceed 60 % for all the board materials). In the same time, the transverse effective permittivity decreases more accentuated and with different slope than the parallel permittivity. This is an indirect effect of the material internal geometry (the relative parallel stratification layers in the substrate materials impose the material anisotropy).

For the glass PTFE and glass PPO resin materials, recommended for double-sided PCB, the parallel effective permittivity evolution *versus* frequency are given in Fig. 5. Two types of PPO board materials were considered: a low Dk type R-4726 and a high Dk type, R-4728, for comparison. All resonances obtained for parallel and transverse permittivities are given in Table 2, in the frequency domain of 0.3–7.4 GHz.

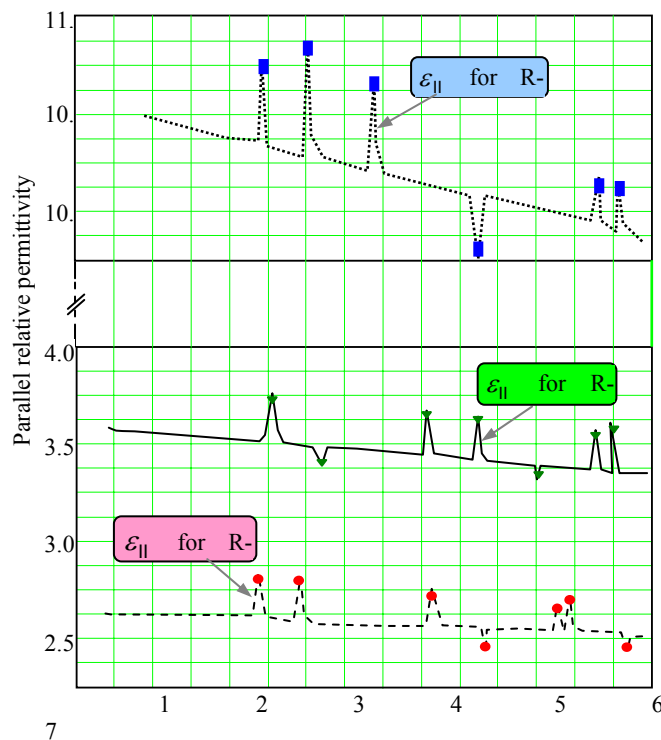


Fig. 5 – The parallel effective permittivities *versus* frequency, for the glass PTFE and glass PPO resin materials, in the frequency range of 0.3-7.4 GHz.

Table 2

Resonant frequencies of the parallel and transverse effective permittivities for the glass PTFE and glass PPO resin materials, in the frequency range of 0.3 - 7.4 GHz

PCB Material	Resonant Frequencies [GHz]	
	Parallel effective permittivity resonances	Transverse effective permittivity resonances
R-4737	2.495; 3.006; 4.712; 5.462; 6.328; 6.504; 7.243	2.862; 3.241; 3.338; 3.503; 4.213; 4.522; 4.769; 4.891; 5.574; 5.673; 6.023; 6.316; 6.641; 6.894; 7.348
R-4726	2.624; 3.286; 4.632; 5.282; 6.093; 6.783; 7.048	3.124; 3.506; 4.302; 4.588; 5.097; 5.703; 6.397; 6.963; 7.086; 7.385
R-4728	2.157; 2.764; 3.721; 5.193; 6.802; 7.143	3.257; 3.502; 3.653; 4.325; 4.749; 5.082; 5.518; 6.429; 6.645; 7.165; 7.423

Legend:
 ● resonances of $\epsilon_{||}$
 ▼ resonances of ϵ_{\perp}

For these categories of materials, resonances number is lower. This is the consequence of a superior grade of homogeneity in comparison with the previous materials. This homogeneity is due to the glass reinforcement and to resin nature.

For the PCB substrate materials, the resin and reinforcement material contents modification determines electrical permittivity variation and changes the resonances [2, 3, 10]. Our method allows us to find the new resonances pattern for different materials compositions. We have exemplified here with the results obtained for the glass thermosetting PPO resin copper-clad laminate R-4726, for different resin contents (Fig. 6).

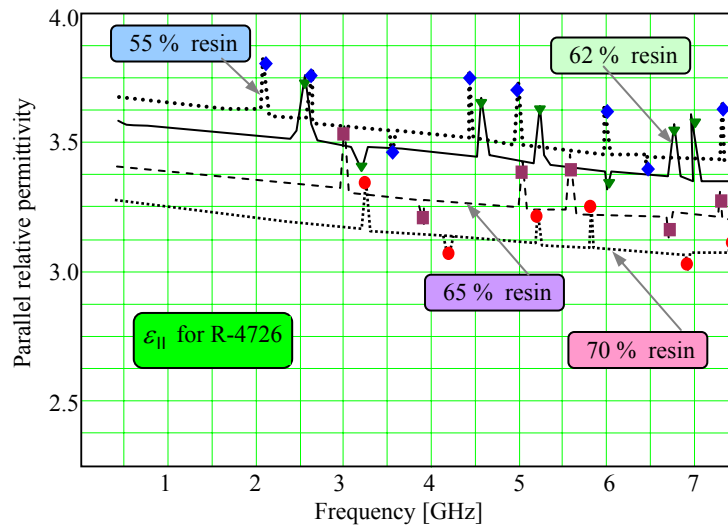


Fig. 6 – The parallel effective permittivity *versus* frequency, for the glass PPO resin material R-4726, for different resin contents.

One observes that the effective permittivity decreases when resin content increases, the material being more hard to be polarized in this case (resin viscosity embarrasses the dipoles movement). In the same time, resonances move to higher frequencies, corresponding to higher energy fields, and resonances number decrease, due to the dipole orientation difficulties.

Tables 1 and 2 indicate us that in case of double-sided PCB materials resonances appear at higher frequencies than in the case of the materials for multi-layer PCB. This is an advantage for these materials exploitation and is determined by the nature of material reinforcement (glass fiber here, with lower values for geometrical parameters corresponding to the resonant frequencies [2]), in association with the resin nature.

The resonant frequencies of every material depend on its components nature and geometry and do not depend on exposure field characteristics [3, 8]. That is why our testing field has not to reproduce exactly the inhomogeneous field configuration, where a real PCB works. This is another advantage of the method.

4. CONCLUSIONS

PCB substrate materials with good HF behavior, used for lead-free design, were analyzed in this paper and their electric properties were illustrated by effective permittivity determinations, in microwave range. The resonant frequency behavior of this quantity was illustrated for every analyzed anisotropic material. Resonances of the permittivity components ε_{\parallel} and ε_{\perp} were determined and their position on frequency scale was linked by material characteristics and interaction process with the testing field. The following conclusion can be drawn, as well:

- Our CAD technique for permittivity determination based on energetic considerations is a flexible method, applicable to many categories of PCB materials. The most important advantage of the method is resonance determination, which can not be illustrated by other classical methods.

- Another advantage of the method is the determination of every permittivity tensor component; this individual determination is very difficult to be done by other methods.

- Resonance patterns, presented separately for parallel and transverse permittivities, offer us the possibility to discern about optimal PCB sample orientation in a surrounding electromagnetic field.

- Comparing different materials resonances pattern, one discerns on the convenient material for a given application, to avoid working at critical (resonant) frequencies. In the same time, materials with a lower number of resonances can be selected.

- Influence of different physical and geometrical parameters on resonances pattern can be illustrated and controlled resonances modification can be induced in this way.

- Resonances pattern depends strongly on reinforcement material and resin nature. For a defined composed material, increasing the resin content determines permittivity modification (decreasing for the most of frequently used materials). In the same time, resonances moves to higher frequencies, their spacing increases and their number even decreases when the resin content increases more than a few percents.

REFERENCES

1. J. H. Lau, C. P. Wong, N. C. Lee, and R. Lee, *Electronics Manufacturing with Lead-Free, Halogen-Free, and Conductive Adhesive Materials*, McGraw-Hill Book Company, New York, 2003.
2. B. P. Scaife, *Principles of Dielectrics*, Clarendon Press, New York, Oxford University Press, 1998.
3. R. E. Camley, *J. Appl. Phys.*, **82**(6), 3058-3067 (1997).
4. J. Wang (ed.), *Design of Experiments for Lead-free Soldering*, Book Chapter Environment Friendly Electronics: Lead-Free Technology, Electrochemical Publications Ltd., 2001.

5. S. Lefrancois, *Modélisation et mesure des propriétés radioélectriques de matériaux hétérogènes en ligne de transmission*, Ph.D. Thesis, Université Paris 6, 1995.
6. *** <http://209.85.129.132/search?q=cache:gDecAPN627wJ:www.matrixusa.us/pdfs/Data%2520Sheet%2520Megtron6.pdf+Megtron&hl=ro&ct=clnk&cd=5&gl=ro>
7. *** http://209.85.129.132/search?q=cache:dcPkyCIKHAKJ:pewkr.panasonic.co.kr/product/pdf_elec/R5715T.pdf+Megtron+Plus+R-5715T&hl=ro&ct=clnk&cd=4&gl=ro
8. D. Ionescu, B. Ciobanu, I. Radinschi, *J. Optoelectron. Adv. M.* **9**, 8, 2608–2616 (2007).
9. D. Ionescu, B. Ciobanu, *J. Optoelectron. Adv. M.*, **10**, 12, 3416–3425 (2008).
10. J. L. Grenestedt and P. Hutapea, *J. Appl. Phys.*, **94**, 1, 686–696 (2003).
11. S. Zhao, G. Li, A. Ding, T. Wang and Q. Yin, *J. Phys. D: Appl. Phys.*, **39**, 2277–2281 (2006).
12. N. Tigau, *Romanian Journal of Physics*, **53**, 203–208 (2008).
13. D. Ionescu, P. Duma, *Proc. 12th Int. Symp. for Design and Technology of Electronic Packages*, Sept. 21–24, 2006, Iasi, Romania, 2006 pp. 34–38.
14. *** *Generic Standard on Printed Board Design*, IPC-2221 A, Association connecting electronics industries.
15. *** *Sectional Design Standard for Rigid Organic Printed Board*, IPC-2222.